JOURNAL OF MATERIALS SCIENCE 32 (1997) 4429–4435

Nickel and copper deposition on Al_2O_3 and SiC particulates by using the chemical vapour deposition–fluidized bed reactor technique

CHIH-CHI CHEN, SINN-WEN CHEN*
Department of Chemical Engineering, National Tsing-Hua University Hsin-Chu, Taiwan 30043

A chemical vapour deposition–fluidized bed reactor technique was developed to perform metal deposition on ceramic particulates. Experiments of nickel and copper deposition on Al_2O_3 and SiC particulates were conducted. Argon was used as the carrier gas to fluidize the ceramic particulates. The metal–H–Cl system was selected for the chemical vapour deposition. The volumetric ratios of the inlet gas were 3.5% HCl, 20.0% H_2, and 76.5% Ar. The deposition reactions were carried out at four different temperatures: 500, 600, 700 and 800 °C. Successful deposition of metallic nickel and copper on the ceramic particulates was observed. It was also noticed that the deposition rates varied with the types of substrates and deposited metals.

1. Introduction

Alumina and SiC particulates are the most often used reinforcing materials in the aluminium-based metal matrix composites. However, wetting between the particulates and the molten aluminium is poor. Attempts, such as adding an active element to the aluminium alloys, or surface treatment of particulates, have been made to enhance their wettability. The addition of active elements also increases the interfacial instability between the alloy and the reinforcing materials, and decreases the reliability of the composites. Therefore, surface treatment of the reinforcing particulates should be a better approach. Layer of nickel and copper on the ceramic particulates have been found to be effective in increasing their wettability with the molten aluminium alloys [1–4].

Wet methods, such as the sol–gel process and the electroless plating process, have been used in the surface treatment of these ceramic particulates. The prominent chemical vapour deposition (CVD) method [5], which has recently gained the most important application in the integrated circuit (IC) industry, has been used in the surface treatment of reinforcing fibres [2]. Compared with the wet method, the usage of the dry method has at least two advantages: it does not require any solvent, and its product usually has a higher degree of cleanliness. However, the high-vacuum type CVD is costly, and the handling of particulates inside the high-vacuum chamber is, indeed, very difficult.

The fluidized bed coating process was developed as early as 40 years ago, mostly in polymer coating without chemical reactions being involved [6, 7]. Although the chemical vapour deposition-fluidized bed reactor (CVD–FBR) technology was developed and used in the coatings of nuclear fuels in the 1960s [8], little attention focused on this technology until the late 1980s. A list of the investigations concerning CVD–FBR is given in Table I [8–24]. Sanjurjo *et al.* proposed a method of metal deposition by using CVD–FBR, and were awarded a patent for such a technique [13, 16–20]. The conventional CVD reactor has at least two different zones: the vaporization zone and the deposition zone. The most significant part of Sanjurjo *et al.*'s design is the *in situ* production of the deposition precursor, and thus the distinction between the two zones no longer existed. As can be noticed in Table I, the reaction temperature can be reduced owing to the *in situ* production of the deposition precursor. Most of the work CVD–FBR work by Sanjurjo *et al.* [13, 16–20] was focused on deposition of aluminium, titanium and silicon on bulk substrates, and is summarized in Table II. Their metal powders were fluidized while the bulk substrates were immersed in the fluidized bed. In one of their works [18], the substrate was fluidized; however, the precursor was not produced *in situ* in that particular work.

The principal aim of this study was to develop a technique for the deposition of metal on ceramic particulates, while the deposition precursor is produced *in situ*. In this study, the metal particulates were in the packed bed and the ceramic substrates were fluidized. Owing to our interest of aluminium-based metal matrix composites, nickel and copper were selected to perform deposition on the Al_2O_3 and SiC

* Author to whom all correspondence should be addressed.

0022–2461

TABLE I A list of the previous CVD–FBR investigations

Year	Coatings	Precursors	Reference	Temperature(°C)
1966	SiC	$SiHCl_3$, CH_4	Blocher [8]	
1975	Pyrolytic carbon	Hydrocarbons	Guilleray *et al.* [9]	1200–2000
1975	Ni	$Ni(CO)_4$	McCreary [10]	112–122
	Mo	$Mo(CO)_6$		352
	Re	$Re_2(CO)_{10}$		352
1975	TiC	$TiCl_4$, C_7H_8	Arthur and Johnson [11]	1200
1988	ZrC	$ZrCl_4$, hydrocarbons	Kaae [12]	
	Co	CoI_2, hydrocarbons		
	HfC	$HfCl_4$, hydrocarbons		
1989	Si	Si, HBr	Sanjurjo *et al.* [13]	600–750
	Ti	Ti, HBr		750
	Zr	Zr, HBr		900
1989	TiN	$TiCl_4$, NH_3	Morooka *et al.* [14]	700–900
1991	AlN	$AlCl_3$, NH_3	Kimura *et al.* [15]	800–1100
1991	Ti	Ti, HCl	Sanjurjo *et al.* [16]	627
	Si	Si, HCl	Sanjurjo *et al.* [17]	350–600
	Al	Trimethylaluminium	Wood *et al.* [18]	200–300
1992	Al	Al, HCl	Lau *et al.* [19]	487
1993	TiN	$TiCl_4$, NH_3	Tsugeki *et al.* [21]	700
1994	TiC	Ti, NH_4Cl	Kinkel *et al.* [22]	
1994	C(Carburizing)	Hydrocarbons	Reynoldson [23]	
	N(Nitriding)	NH_3		
1995	N(Nitriding)	N_2, NH_3	Chang *et al.* [24]	1000–1300

TABLE II Comparsion of the work of Sanjurjo *et al.* and this study

	This study	Sanjurjo *et al.*
Coating elements	Ni, Cu, Ti	Al, Ti, Si
State of the coating sources	Metal pellets in the fixed bed	Metal powders in the fluidized bed
State of the substrates	Particulates in the fluidized bed	Bulks immersed in the fluidized bed
Reactive gases	HCl, H_2	HCl (or HBr), H_2
Generation of the coating precursors	*In situ*	*In situ*

particulates. Based on the knowledge of related studies on similar systems and the thermodynamic properties in the literature [16–20, 25–28], the metal–H–Cl system was selected to perform the metal deposition, i.e. pure metal, HCl gas and H_2 gas were used.

2. Experimental procedure

As shown in Fig. 1, the apparatus for the CVD–FBR experiment consisted of three major parts: the gas inlet, the furnace, and the quartz reactor. The quartz reactor was installed inside a vertical tube furnace. The inside diameter (i.d.) of the furnace tube was 2.54 cm and the height of the furnace was 30 cm. The outside diameter (o.d.) and i.d. of the quartz reactor were 2.2 and 2.0 cm, respectively. A close-up of the quartz reactor is shown in Fig. 2. The metal-packed bed was 3 cm high and was located on top of the quartz distributor plate. The ceramic particulate substrates for deposition were loaded on top of the metal-packed bed. The size of the ceramic particulates was 250 μm diameter. Ceramic particulates of this size are too large to be used practically in the metal matrix composites. However, detailed analysis of the deposits on fine particulates is difficult, and it is not easy to fluidize finer particulates by using conventional FBR.

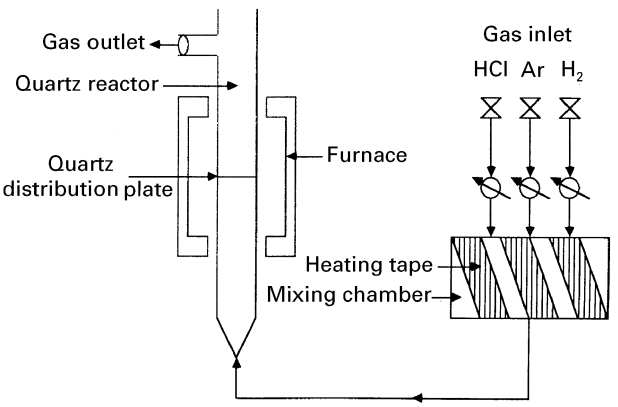

Figure 1 A schematic diagram of the CVD–FBR apparatus used in this study.

The principal goal of this study was to develop a new technique to deposit metal on ceramic particulates, while the deposition precursor is produced *in situ*. Attempts were then made to modify the fluidized bed reactor so that much finer particulates could be handled. In fact, a floating type reactor proposed by Kimura *et al.* [15] has demonstrated the feasibility of handling very fine particulates, and the use of that type of FBR in the metal deposition on fine ceramic particulates will be investigated in the future. Besides

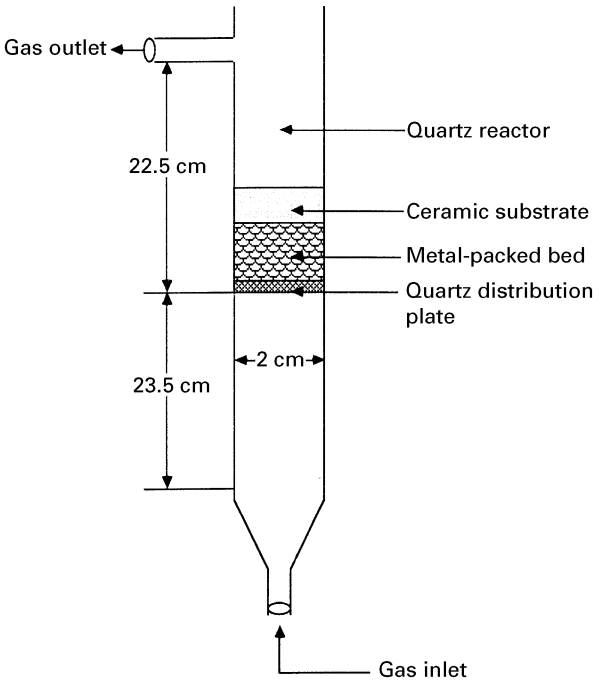

Figure 2 A schematic diagram of the quartz reactor.

the ceramic particulates, other bulk substrates, such as alumina plate, copper plate and stainless steel wire, which were also investigated in this study, were suspended on top of the metal bed.

The quartz reactor was then loaded inside the furnace and heated to the predetermined temperature. The argon gas was first introduced into the reactor to fluidize the ceramic particulates. After the system became stabilized, hydrogen and hydrogen chloride gases were then introduced. The minimum fluidization gas velocities (u_{mf}) for Al_2O_3 and SiC particulates were estimated as 9.1 and 7.7 cm s^{-1}, respectively, using the following equation, proposed by Chitester *et al.* [29].

$$Re_{p,mf} = [(28.7)^2 + 0.0494Ar]^{1/2} - 28.7 \quad (1)$$

where $Re_{p,mf}$ and Ar are the Reynolds number of minimum fluidization and Archimedes number, respectively. These are defined by Kunii and Levenspiel [29]: $Re_{p,mf} = du_0\rho_g/\mu$ and $Ar = d^3\rho_g(\rho_s - \rho_g)g/\mu^2$ where d is particle diameter, u_0 superficial gas velocity, ρ_g gas density, ρ_s solid density. The calculated values were close to the experimentally determined results, 10 and 9 cm s^{-1} for Al_2O_3 and SiC particulates, respectively. The velocity of the mixed reaction gas in these CVD–FBR experiments was 12.5 cm s^{-1}, which was higher than u_{mf}. At this gas velocity, the reactor was operating in the bubble bed regime.

The three different gases (argon, H_2 and HCl) were mixed and pre-heated to 250 °C in the mixing chamber. The pre-heated reaction gas was then passed through the distributor, into the metal-packed bed, and reacted with the metal pellet to form the deposition precursor. The precursor was carried into the fluidized bed by the remaining gas; it then decomposed and the metal was deposited on the ceramic particulates. An hour later, the HCl gas was turned off first; the hydrogen and argon continued flowing to make sure there were no HCl or Cl_2 gases left in the system. Then the hydrogen gas and the furnace were turned off. The argon gas purge continued until the furnace had cooled down. The metal-deposited substrates were then removed from the reactor. The products were analysed by using optical microscopy (OM), scanning electron microscopy (SEM), energy dispersive spectrometry (EDS), and X-ray diffractometry (XRD). The thickness of the deposition layers of some products was calculated from the results of density measurements.

3. Results and discussion

3.1. Nickel deposition

Nickel deposition using CVD was first explored by Mond [30] as early as 1889, and has been widely investigated since then [30–34]. Ihara *et al.* [35] studied the reactions between metallic nickel and HCl gas, and they found yellow-coloured $NiCl_2$ solid formed at 400 °C; however, no appreciable amount of $NiCl_2$ sublimate was formed until the temperature exceeded 500 °C. Because deposition in this study was carried out in the gas phase, experiments were all conducted at temperatures equal to or higher than 500 °C, namely at 500, 600, 700, and 800 °C.

However, no nickel deposit was observed on either the ceramic substrates or the inner wall of the quartz reactor for the CVD–FBR experiments conducted at 500 °C. For the experiments conducted at 600 °C, yellow-coloured deposits were noticed on the inner wall of the quartz reactor. The XRD pattern shown in Fig. 3 indicates that those deposits were $NiCl_2 \cdot 6H_2O$. This result is in agreement with the results in the literature [35] that at 600 °C the reaction product between HCl and nickel was $NiCl_2$. It is presumed that the $NiCl_2$ absorbed moisture and formed $NiCl_2 \cdot 6H_2O$ during handling. On the basis of the experimental observations and data in the literature [26, 27, 35], it can be presumed that the deposition precursor was $NiCl_2$. This deposition precursor was carried by the gas stream into the fluidized bed, then decomposed, and nickel was deposited on the alumina particulates.

After the deposition experiments at 700 °C with CVD–FBR, the colour of the originally white alumina particulates turned brownish. Compositional analysis

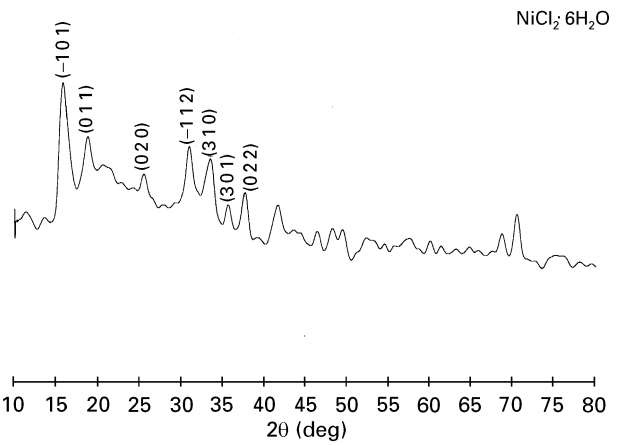

Figure 3 XRD pattern of the yellow-coloured deposits on the inner wall of the reactor from the 600° C nickel-deposition experiment.

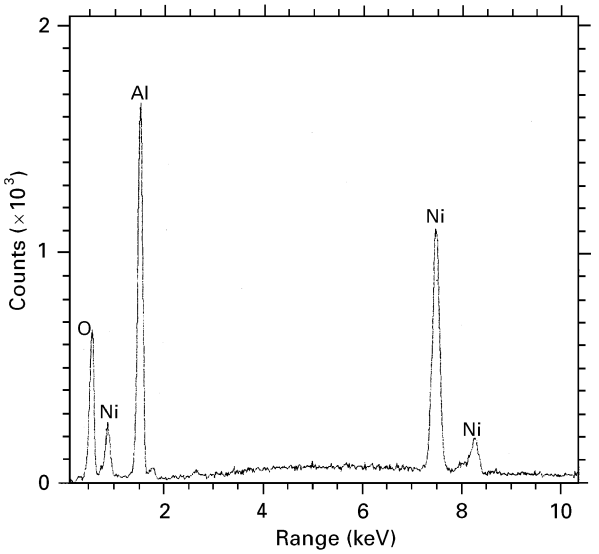

Figure 4 EDS result of the nickel-deposited alumina particulates from the 700° C experiment.

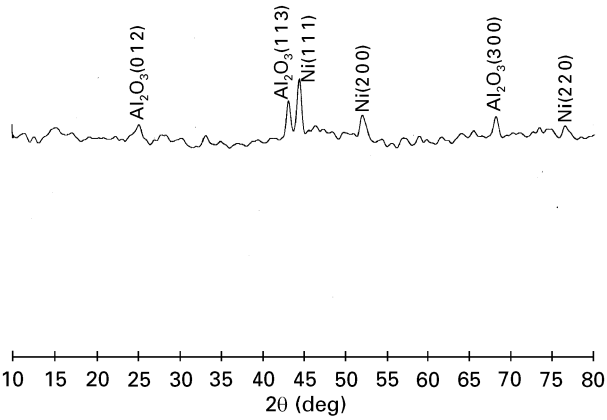

Figure 5 XRD pattern of the nickel-deposited alumina particulates from the 700° C experiment.

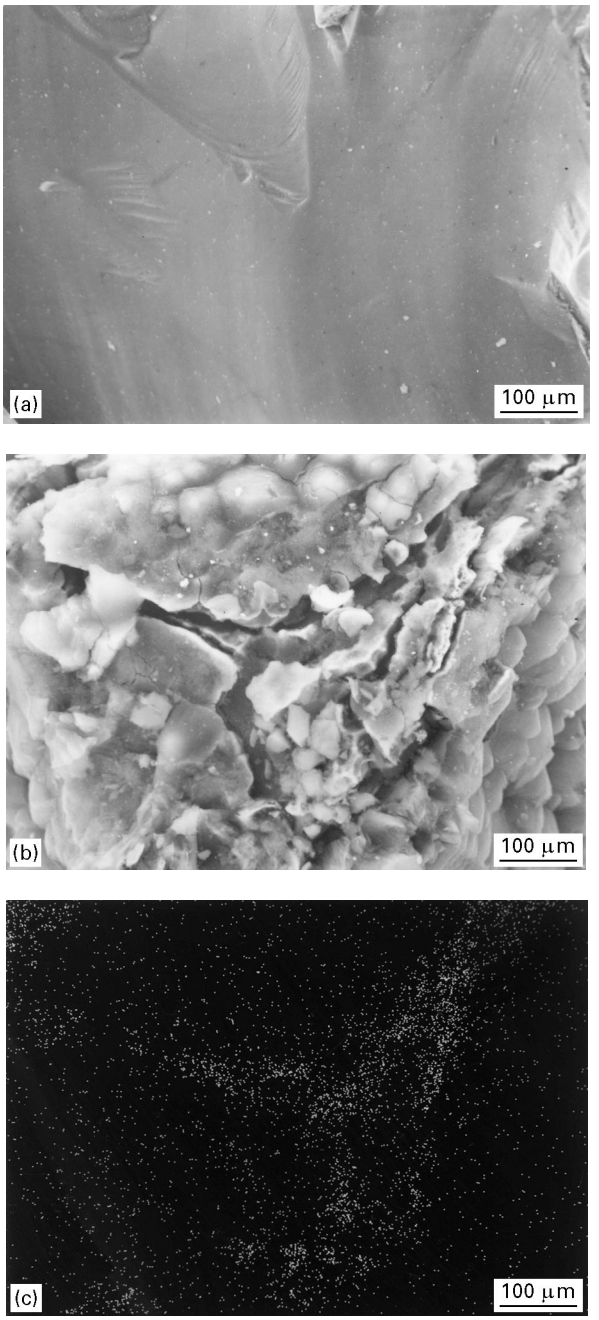

Figure 6 Scanning electron micrograph of the alumina particulates in the as-received condition. (b) Scanning electron micrograph of the nickel-deposited alumina particulates removed from the 700° C CVD–FBR experiment. (c) Nickel elemental X-ray mapping of the nickel deposited alumina particulates removed from the 700° C CVD–FBR experiment.

of the brownish particulates was carried out by using energy-dispersive spectrometry (EDS). The EDS result is shown in Fig. 4, in which the elements of aluminium, nickel and oxygen were identified. Metallic nickel phase and alumina phase were the only two phases observed by using XRD analysis, as shown in Fig. 5. The EDS and XRD results demonstrated that metallic nickel was successfully deposited on the alumina particulates by using this CVD–FBR technique conducted at 700 °C. The surface morphology of the alumina prior to and after the nickel-deposition was examined using SEM and is shown in Fig. 6a and b, respectively. A nickel elemental X-ray mapping of the deposited alumina is also shown in Fig. 6c. It can be noticed in Fig. 6b that the deposited nickel was plate-like. This observation was also true of the reactions at 800 °C. For the same reaction time, the peak intensities of nickel from the 800 °C experiment determined by both the EDS and XRD results were stronger than those from the 700 °C experiment, which indicated that the amount of deposition of metallic nickel increased with reaction temperature. The deposition rates at 700 °C were approximated by an indirect method using density measurements. The determined densities of alumina and nickel-deposited alumina were 4.0 and 4.4 g cm^{-3}, respectively. By assuming the particulates to be uniform spheres of 250 μm diameter, and by assuming a dense and uniform nickel deposit, the thickness of the nickel coating and the nickel-deposition rate on the alumina particulates were calculated to be 3.6 μm and 7.7 mg cm^{-2} h^{-1}, respectively. This deposition rate was slightly higher than the rate of electroless nickel-plating on alumina plate, 4.2 mg cm^{-2} h^{-1}, which was conducted at 80 °C [36].

Efforts to deposit nickel on the SiC particulates were carried out in the same manner as the deposition

TABLE III Thickness of the deposition layer calculated via density measurement. All the deposition experiments were conducted at 700° C for 1 h

Samples	Densities ($g\,cm^{-3}$)	Thickness (μm)
Al_2O_3	4.0	–
SiC	3.3	–
Ni/Al_2O_3	4.4	3.6
Ni/SiC	3.6	2.1
Cu/Al_2O_3	5.0	9.4
Cu/SiC	4.1	6.2

on the alumina particulates, and similar results were obtained. At 500 and 600 °C, no nickel deposits were found on the surface of the SiC particulates. At 700 °C, metallic nickel element could be found on the alumina, and its morphology was plate-like. The amount of nickel also increased when the temperature was raised to 800°C. With similar assumptions as mentioned above, the thickness of the nickel layer was calculated from the results of density measurements. The thickness was 2.1 μm as given in Table III. The results indicated that deposition rates varied with the type of substrate, even when other operation parameters were kept constant. This phenomenon was further examined by using CVD–FBR to deposit nickel on three other different substrates: alumina plate, copper plate and stainless steel wire. Under identical experimental conditions, much stronger EDS peaks of metallic nickel were always found on the metal substrates when compared with those on ceramic substrates. Although density measurements were not conducted on the metal bulk substrates, the much stronger EDS peaks indicated that the rates of nickel deposition on the metal substrates were much higher than those on Al_2O_3 and SiC.

3.2. Copper deposition

Various investigators have studied copper deposition with the CVD technique using different compounds as the copper source [37–41]. However, research with *in situ* production of the copper-deposition precursor, or research regarding the copper reaction with the HCl gas similar to the study of the Ni–HCl system by Ihara *et al.* [35], are not available in the literature. On the basis of knowledge from related studies and the limited thermochemical properties of the Cu–H–Cl system [26, 27], it was decided that the deposition of copper on ceramic particulates would be carried out in a similar manner to the previous nickel-deposition. Pure metallic copper pellets, HCl and hydrogen gases were used. The reaction temperatures were at 500, 600, 700 and 800 °C.

Similar to the previous nickel-deposition case, no change was observed when the reaction was carried out at 500°C. When the reaction temperature rose to 600 °C, light yellowish deposits were found on the inner wall of the quartz reactor, and a very light orange colour was displayed on the alumina particulates. The light yellowish deposits were scrubbed off the wall and analysed by using XRD. As shown in Fig. 7, the deposit was CuCl, which could be the deposition precursor. A much more complete study about the reaction mechanism still needs to be carried out before a sound conclusion can be drawn. The EDS analysis on these deposits indicated the existence of copper and chlorine elements. After the CVD–FBR experiment at 700 °C, the alumina particulates displayed an orange colour, and copper-like deposits with shiny orange colour were found on the inner wall of the reactor. The XRD analysis of these wall deposits confirmed the existence of metallic copper. The successful deposition of metallic copper on the alumina particulates was confirmed by using EDS and XRD analysis on the orange-coloured substrates. Fig. 8 shows the EDS result, and the existence of copper element can clearly be noticed. Fig. 9 shows the XRD pattern, and peaks of both the metallic copper deposits and the alumina substrates were identified. The surface morphology of the copper-deposited alumina was examined by using SEM and is shown in Fig. 10. It is obvious the morphology of the deposited copper

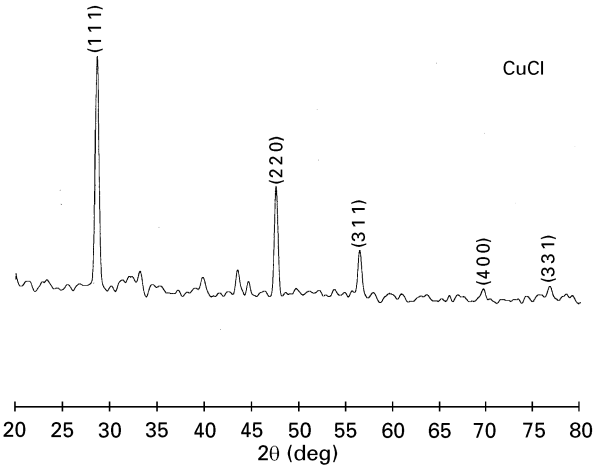

Figure 7 XRD pattern of the wall deposits from the 600° C CVD–FBR experiment for copper deposition.

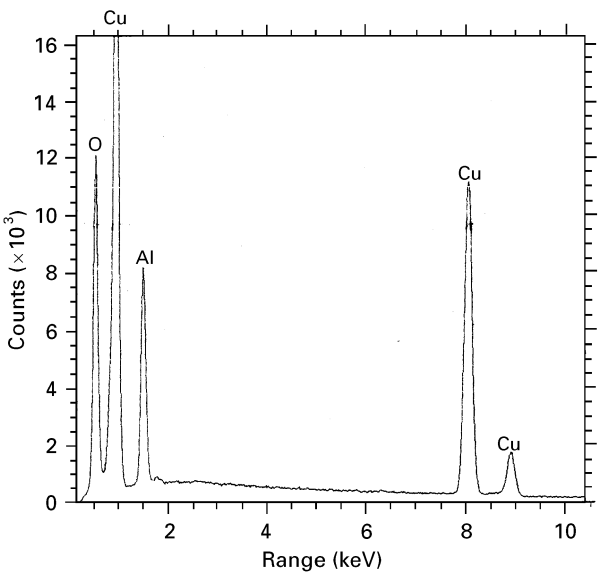

Figure 8 EDS result of the copper-deposited alumina particulates from the 700° C experiment.

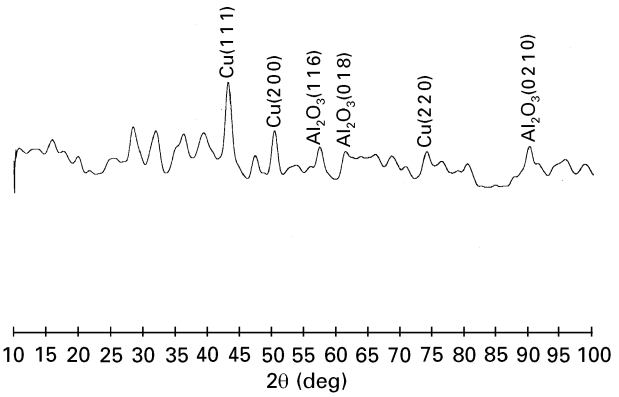

Figure 9 XRD pattern of the copper-deposited alumina particulates from the 700° C experiment.

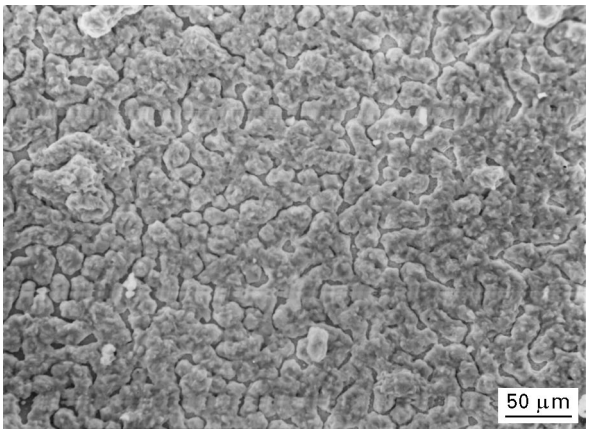

Figure 10 Scanning electron micrograph of the copper-deposited alumina particulates removed from the 700° C CVD–FBR experiment.

is much smoother than that of the deposited nickel. As listed in the Table III, the determined thickness of the copper layer on the alumina particulates was 9.4 μm, and the deposition rate of copper on alumina was faster than that of nickel. The results obtained at 800 °C were similar to those obtained at 700 °C, i.e. metallic copper was found on the alumina particulates and the morphology was smooth as well. However, unlike the nickel deposition case, the amount of copper deposit decreased when the reaction temperature was raised to 800 °C. Severe sintering was observed in the copper-packed bed at 800 °C. The large reduction in the surface area of the copper due to sintering is likely to be the main cause of the decreasing amount of deposits.

Copper deposition on the SiC particulates was conducted in an identical manner to the deposition on the Al_2O_3 particulates, and similar results were also observed. An appreciable amount of metallic copper deposition was found on the substrates deposited at 700 °C. As can be seen in Fig. 11, the morphology of the deposited copper on the SiC particulates is similar to the deposited copper on the alumina particulates, as shown in Fig. 10, and is very different from the deposited nickel on the ceramic particulates as shown in Fig. 6b. It can also be noticed in Table III that the amount of deposited copper on the SiC particulates at

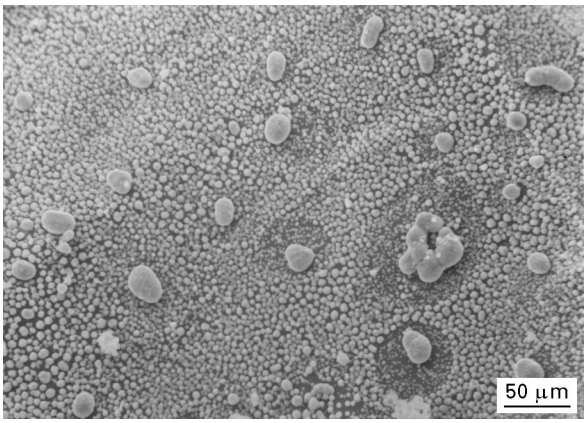

Figure 11 Scanning electron micrograph of the copper-deposited SiC particulates removed from the 700° C CVD–FBR experiment.

700 °C for 1 h reaction was 6.2 μm and was less than that on the alumina, which was in agreement with the observation in the nickel deposition that the deposition rate was higher on the alumina substrate. Experiments of copper deposition on the alumina plate and stainless steel wire were also examined in similar procedures, and the deposition rate of copper on the metal substrate was found to be much higher than that on the alumina.

4. Conclusion

A new CVD–FBR technique was successfully developed to perform metallic nickel and copper deposition on ceramic particulates, while the deposition precursor was *in situ* produced. The formation of nickel and copper deposits on the alumina and SiC particulates was confirmed and the products were analysed. It was observed that the deposition rates increased with reaction temperature, and it was also noticed that the deposition rates varied with types of substrates and deposited metals. The systems arranged in order of deposition rate are: copper and nickel on metal substrates, copper on Al_2O_3, copper on SiC, nickel on Al_2O_3, and nickel on SiC. Although the feasibility of surface treatment of ceramic particulates by using this CVD-FBR technique has been demonstrated, the 250 μm size particulates investigated in this study are too large to be used in the metal matrix composites. Attempts are now being undertaken to modify the fluidized bed reactor following the work of Kimura *et al.* [15] so that much finer ceramic particulates, e.g. with a size of 25 μm diameter, can be handled.

Acknowledgements

The authors thank Professor Shyh-Jye Huang, Professor Kan-Sen Chou, and Dr Hsiu-Mu Tang for many helpful discussions, and also acknowledge the financial support of the National Science Council in Taiwan, under grant NSC-84-2214-E-007-019.

References

1. M. M. SCHWARTZ, "Composite Materials Handbook" (McGraw-Hill, New York, 1982).
2. A. MORTENSEN and I. JIN, *Inter. Mater. Rev.* **37**(3) (1992) 101.
3. C.-L. TSAO and S.-W. CHEN, *J. Mater. Sci.* **30** (1995) 5215.
4. S. L. I. CHAN and C. C. CHANG, in "Proceedings of the 1995 Annual Conference of the Chinese Society for Materials Science", Vol. II, (Chinese Society for Materials Science, 1995) pp. 388–89.
5. P. L. CHEN, *J. Vacuum Soc. ROC* **5**(2) (1992) 4.
6. J. GAYNOR, *Chem. Engng Prog.* **56**(7) (1960) 75.
7. A. H. LANDROCK, *ibid.* **63**(2) (1967) 67.
8. J. M. BOLCHER Jr, US Pat. 3249 509 (1966).
9. J. GUILLERAY, R. L. R. LEFEVRE, M. S. T. PRICE and J. P. THOMAS, in "Proceedings of the 5th International Conference on CVD", edited by J. M. Bolcher Jr, H. H. Hinterman and L. H. Hall (Electrochemical Society, Princeton, NJ, 1975) pp. 727–48.
10. W. J. McCREARY, *ibid*., pp. 714–25.
11. G. ARTHUR and M. P. JOHNSON, *ibid*., pp. 509–22.
12. J. L. KAAE, *Ceram. Engng Sci. Proc.* **9** (1988) 1159.
13. A. SANJURJO, M. C. H. McKUBRE and G. D. CRAIG, *Surf. Coat. Technol.* **39**/**40** (1989) 691.
14. S. MOROOKA, T. OKUBO and K. KUSAKABE, *Powder Technol.* **63** (1990) 105.
15. I. KIMURA, N. HOTTA, J.-I. NIWANO and M. TANAKA, *ibid.* **68** (1991) 153.
16. A. SANJURJO, B. J. WOOD, K. H. LAU, G. T. TONG, D. K. CHOI, M. C. H. McKUBRE, H. K. SONG, D. PETERS and N. CHURCH, *Surf. Coat. Technol.* **49** (1991) 103.
17. A. SANJURJO, B. J. WOOD, K. H. LAU, G. T. TONG, D. K. CHOI, M. C. H. McKUBRE, H. K. SONG and N. CHURCH, *ibid.* **49** (1991) 110.
18. B. J. WOOD, A. SANJURJO, G. T. TONG and S. E. SWIDER, *ibid.* **49** (1991) 228.
19. K. H. LAU, A. SANJURJO and B. J. WOOD, *ibid.* **54**/**55** (1992) 234.
20. A. SANJURJO, US Pat. 5171 734 (1992).
21. K. TSUGEKI, T. KATO, Y. KOYANAGI, K. KUSAKABE and S. MOROOKA, *J. Mater. Sci.* **28** (1993) 3168.
22. S. KINKEL, G. N. ANGELOPOULOS and W. DAHL, *Surf. Coat. Technol.* **64** (1994) 119.
23. R. W. REYNOLDSON, *Ind. Heating* September (1994) 126.
24. A.-J. CHANG, S.-W. RHEE and S. BAIK, *J. Mater. Sci.* **30** (1995) 1180.
25. R. H. BUSEY and W. F. GIAUQUE, *J. Amer. Chem. Soc.* **75** (1953) 1791.
26. M. W. CHASE Jr, J. L. CURNUTT, J. R. DOWNEY Jr, R. A. McDONALD, A. N. SYVERUD and E. A. VALENZUELA, *J. Phys. Chem. Ref. Data* **11** (1982) 695.
27. O. KUBASCHEWSKI, E. LL. EVANS and C. B. ALCOCK, "Metallurgical Thermochemistry" (Pergamon Press, London, 1967) pp. 414–26.
28. D. T. WILLIAMS, S. K. EL-RAHAIBY and Y. K. RAO, *Metall. Trans.* **12B** (1981) 161.
29. D. KUNII and O. LEVENSPIEL, "Fluidization Engineering", 2nd Ed. (Butterworth-Heinemann, Boston, 1991).
30. H. E. CARLTON and J. H. OXLEY, *AIChE J.* **13**(1) (1967) 86.
31. P. J. CLEMENTS and F. R. SALE, *Metall. Trans.* **7B** (1976) 435.
32. T. MARUYAMA and T. TAGO, *J. Mater. Sci.* **28** (1993) 5345.
33. Y. UEMURA, Y. HATATE and A. IKARI, *J. Chem. Engng Jpn.* **22**(1) (1989) 48.
34. L. VAN HEMERT, B. SPENDLOVE and R. E. SIEVERS, *J. Electrochem. Soc.* **112** (1965) 1123.
35. Y. IHARA, H. OHGAME and K. SAKIYAMA, *Corros. Sci.* **22** (1982) 901.
36. K.-L. LIN and C.-S. JONG, *Mater. Chem. Phys.* **35** (1993) 53.
37. D.-H. KIM, R. H. WENTORF and W. N. GILL, *J. Electrochem. Soc.* **140** (1993) 3267.
38. B. LECOHIER, J.-M. PHILIPPOZ and H. VAN DEN BERGH, *J. Vac. Sci. Technol. B* **10** (1991) 262.
39. R. KUMAR, F. R. FRONCZEK, A. W. MAVERICK, W. G. LAI and G. L. GRIFFIN, *Chem. Mater.* **4** (1992) 577.
40. V. L. YOUNG, D. F. COX and M. E. DAVIS, *ibid.* **5** (1993) 1701.

Received 4 December 1995
and accepted 10 February 1997